






Toward coherent anti-Stokes Raman scattering-Raman optical activity for reaction monitoring in organocatalysis: Chiral vibrational signatures of the two atropisomers (*R*)- and (*S*)-MOM-BINOL in solution

Vikas Kumar¹  | Till Reichenauer¹ | Luca Supovec¹ | Dennis Jansen² | Nikolai Brodt² | Grzegorz Zając³  | Agnieszka Domagała^{3,4}  | Małgorzata Barańska^{3,5}  | Jochen Niemeyer² | Sebastian Schlücker¹ 

¹Physical Chemistry I, Department of Chemistry and Center for Nanointegration Duisburg-Essen (CENIDE) and Center for Medical Biotechnology (ZMB), University of Duisburg-Essen, Essen, Germany

²Organic Chemistry, Department of Chemistry and Center for Nanointegration Duisburg-Essen (CENIDE), University of Duisburg-Essen, Essen, Germany

³Jagiellonian Centre for Experimental Therapeutics (JCET), Jagiellonian University, Krakow, Poland

⁴Doctoral School of Exact and Natural Sciences, Jagiellonian University, Krakow, Poland

⁵Faculty of Chemistry, Jagiellonian University, Krakow, Poland

Correspondence

Vikas Kumar and Sebastian Schlücker, Physical Chemistry I, Department of Chemistry and Center for Nanointegration Duisburg-Essen (CENIDE) and Center for Medical Biotechnology (ZMB), University of Duisburg-Essen, Universitätsstrasse 5, 45141 Essen, Germany.
Email: vikas.kumar@uni-due.de and sebastian.schluecker@uni-due.de

Funding information

Deutsche Forschungsgemeinschaft, Grant/Award Numbers: project number 511625800, 511625800

Abstract

Coherent anti-Stokes Raman scattering-Raman optical activity (CARS-ROA) is a coherent version of spontaneous ROA spectroscopy, the latter being a well-established chirally sensitive vibrational spectroscopic technique. A central major advantage of heterodyne-detected CARS-ROA over ROA is the drastic reduction of acquisition times from several hours to approximately 1 min due to the high ratio of the chiral Raman signal relative to the achiral CARS background. Here, we present the first demonstration of heterodyne-detected CARS-ROA of chiral molecules dissolved in an achiral solvent by using an experimental setup built from a conventional broadband CARS spectrometer. Specifically, the two atropisomers (*R/S*) of 2,2'-Bis(methoxymethoxy)-1,1'-binaphthyl, a methoxymethyl (MOM) bis-protected derivative of 1,1'-Bi-2-naphthol (BINOL), dissolved in the achiral organic solvent dichloromethane (DCM) were characterized by employing ~ 1 ps, 1 mW of pump pulses and ~ 60 fs, 10 mW of Stokes pulses within approximately 4-min acquisition time. MOM-BINOL is an important precursor for the synthesis of a great variety of many chiral auxiliaries including binaphthyl phosphoric acids, which are an important class of chiral organocatalysts used in asymmetric reactions. Overall, this work is a first step toward kinetic reaction monitoring in organocatalysis by coherent ROA providing the necessary short acquisition times.

KEYWORDS

CARS-ROA, chiral Raman, coherent ROA, nonlinear Raman optical activity, Raman optical activity, vibrational Raman spectroscopy

This is an open access article under the terms of the [Creative Commons Attribution-NonCommercial](https://creativecommons.org/licenses/by-nc/4.0/) License, which permits use, distribution and reproduction in any medium, provided the original work is properly cited and is not used for commercial purposes.

© 2023 The Authors. *Journal of Raman Spectroscopy* published by John Wiley & Sons Ltd.

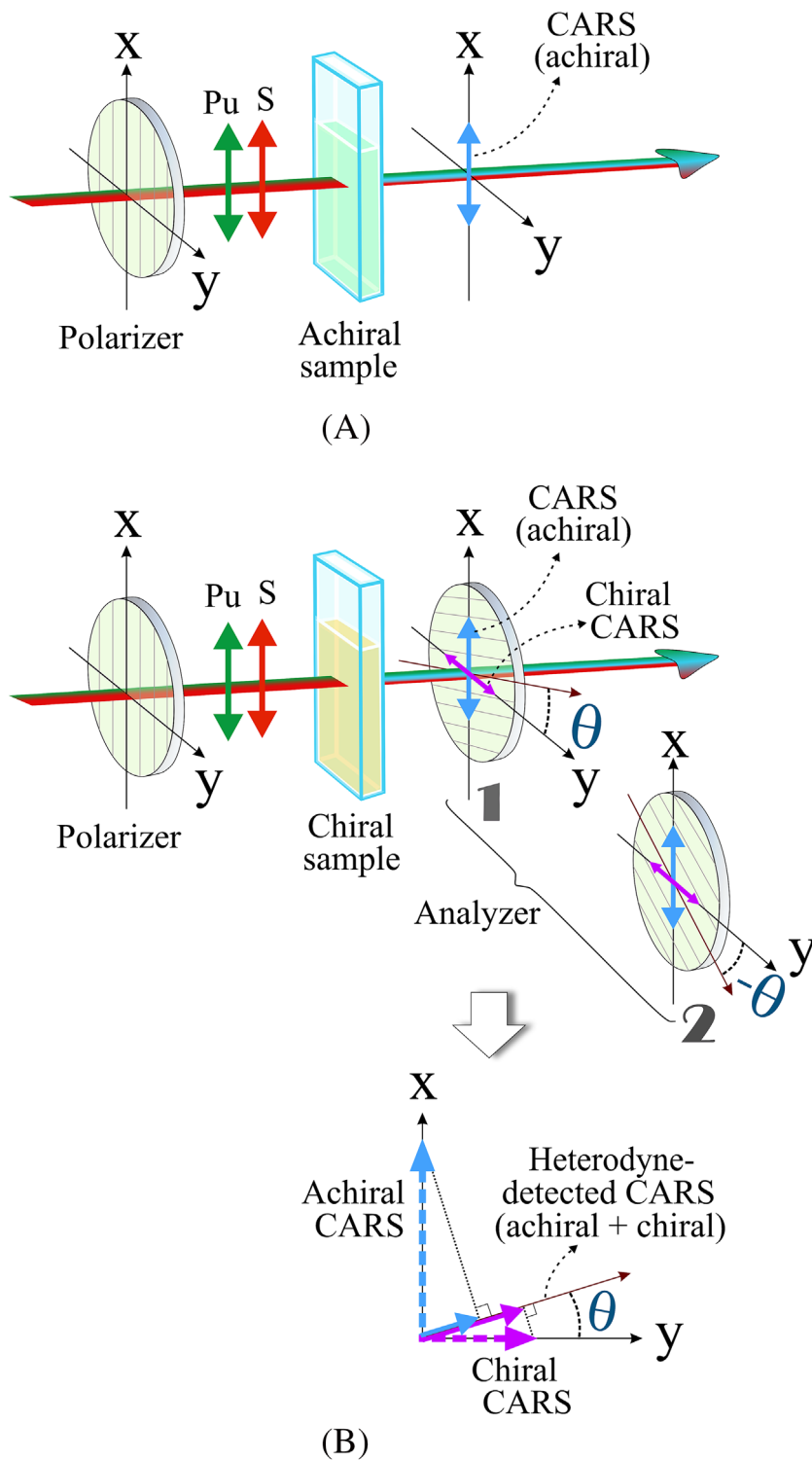
1 | INTRODUCTION

Vibrational optical activity (VOA) is an optical property of chiral molecules that provides enantio-sensitivity and has been exploited for conformational identification and vibrational analysis of chiral molecules in organic chemistry and biochemistry. The two well-established VOA techniques are vibrational circular dichroism (VCD)^{1,2} and Raman optical activity (ROA)^{3–5} spectroscopies. Both VCD and ROA provide more detailed structural information as compared with electronic optical activity methods such as electronic CD and optical rotatory dispersion (ORD), but they require significantly longer acquisition times of up to several hours. On the other hand, many chemical processes involving chiral molecules are much faster. For example, asymmetric organocatalysis,^{6–9} an environment-friendly and sustainable way of synthesizing chiral molecules in which chiral products are obtained from prochiral educts in the presence of a chiral organocatalyst, usually has reaction times in the range of minutes to hours (depending on the catalyst loading). The development of novel asymmetric organocatalytic reactions demands a mechanistic understanding of the pathway(s) involving the chiral catalyst. This calls for a sufficiently fast “time-resolved chiro-sensitive molecular detection” technique that can selectively follow the evolution of molecular chiral structure in the course of the reaction. In comparison with other time-resolved methods such as NMR, ROA not only offers complementary structural information but also enables specific detection of chiral catalysts, intermediates, and products, whereas achiral starting materials and/or solvents are ROA-silent. *En route* to this, nonlinear vibrational ROA techniques such as coherent anti-Stokes Raman scattering-Raman optical activity (CARS-ROA) spectroscopy have the potential to fulfill this demand. These chiro-sensitive nonlinear Raman techniques—due to the coherent nature of their parent technique, for example, CARS—enable an enhancement of the chiral signal by many orders of magnitude as compared to spontaneous ROA signals. Therefore, the acquisition time in these techniques is significantly reduced from hours, as required in conventional ROA, to less than a minute. As a direct counterpart of the spontaneous ROA-circular intensity difference (CID) spectroscopy, CARS-ROA CID has been theoretically predicted to be only nearly 10^{-3} times the achiral CARS background intensity.¹⁰ The spontaneous ROA CID signal is also 10^{-3} times the Raman signal intensity.^{3,11,12} However, the significantly higher signal levels of CARS as compared with spontaneous Raman scattering are supposed to make CARS-ROA CID signals many orders of magnitude stronger than

those of ROA CID. However, CARS-ROA CID has not yet been demonstrated experimentally. On the other hand, thanks to the freedom of polarization configurations in CARS, another “polarization-resolved” CARS-ROA technique called heterodyne-detected CARS-ROA was theoretically proposed by Oudar et al.¹³ in 1982 that can significantly improve the CARS-ROA signal-to-achiral CARS background ratio. The first experimental demonstration of heterodyne-detected CARS-ROA, using a neat chiral liquid, was reported in 2012 by Hiramatsu et al.¹⁴ Specifically, the authors showed for liquid (–)- β -pinene that the CARS-ROA signal-to-achiral CARS background ratio is two orders of magnitude better than the corresponding spontaneous ROA-to-Raman signal ratio. Another advantage of CARS-ROA techniques over spontaneous ROA is that due to the anti-Stokes detection, it is immune to fluorescence and can be applied to study chiral fluorophores where spontaneous ROA might face challenges.

In contrast to the circularly polarized input beams needed in CID measurements, the heterodyne-detected CARS-ROA setup utilizes two collinear input beams with parallel linear polarization; hence, it can be built upon a conventional CARS setup (shown in Figure 1A). The scheme of heterodyne-detected CARS-ROA setup is depicted in Figure 1B. Briefly, two temporally synchronized and linearly polarized (along X-axis) collinear input beams called pump (Pu, frequency ω_{pu}) and Stokes (S, frequency ω_S) irradiate the chiral sample. When their optical frequency difference matches a vibrational mode Ω of the molecules ($\omega_{pu} - \omega_S = \Omega$), and considering beyond the electric dipole approximation and including the electric quadrupole and magnetic dipole interactions, this excitation invokes two types of signal fields at anti-Stokes frequency ($\omega_{aS} = 2\omega_{pu} - \omega_S$). One along the input field polarization, giving rise to conventional CARS (achiral in nature), which is proportional to the third-order susceptibility $\chi_{1111}^{(3)}$, and the other one in the orthogonal polarization direction, giving rise to CARS-ROA (chiral CARS), which is proportional to the third-order susceptibility $\chi_{2111}^{(3)}$. For such linear input polarizations, the CARS-ROA-to-achiral CARS ratio was predicted to be $\sim 10^{-6}$ and it can be further improved up to 10^{-3} for heterodyne detection.¹³ For the latter, a polarizer (analyzer) is inserted after the sample in crossed position (“zero position” where maximum extinction occurs for anti-Stokes field) to completely block the achiral CARS, and then its polarization axis is slightly rotated by a small angle θ to pass a tiny amount of achiral CARS. In this way, the CARS-ROA signal interferes with this achiral CARS leakage to give an overall spectrum represented by $I(\omega_{aS}, \theta)$:

FIGURE 1 Experimental configurations of (A) conventional CARS and (B) heterodyne-detected CARS-ROA.



$$I(\omega_{aS}, \theta) \propto \left[\cos^2 \theta \left| \chi_{2111}^{(3)} \right|^2 + \sin^2 \theta \left| \chi_{1111}^{(3)} \right|^2 + 2 \cos \theta \sin \theta A \cdot \frac{I_{CID}^{sp, ROA}(0^\circ) \cdot \chi_{1111}^{(3)eff, NR} \cdot N \Gamma / 2}{2 \hbar \left\{ (\Omega - \omega_{pu} + \omega_S)^2 + \Gamma^2 \right\}} \right] \quad (1)$$

Here, A is a constant, Γ is a phenomenological damping constant, N is the molecular number density, and $\chi_{1111}^{(3)NR}$ is the non-resonant part of the corresponding susceptibility tensor component. $I_{CID}^{sp, ROA}(0^\circ)$ is the forward scattering spontaneous ROA CID intensity. The details of the derivation can be found elsewhere.^{14,15} The first two terms on the right-hand side of Equation (1) are

homodyne terms, whereas the third term—due to the presence of $I_{CID}^{sp, ROA}(0^\circ)$ —provides the spontaneous ROA-like spectral profile amplified by the non-resonant part $\chi_{1111}^{(3)NR}$ of the achiral CARS. Two such spectra are recorded at $\pm\theta$ angles around the “zero position” with $\theta = 0^\circ$. The difference of the two spectra eliminates the homodyne terms and constitutes the heterodyne-detected CARS-ROA spectrum given by the following expression:

$$\Delta I(\omega_{as}) \equiv I(\omega_{as}, \theta) - I(\omega_{as}, -\theta) \\ \propto 4 \cos\theta \sin\theta A \cdot \frac{I_{CID}^{sp, ROA}(0^\circ) \cdot \chi_{1111}^{(3)NR} \cdot N\Gamma/2}{2\hbar \left\{ (\Omega - \omega_{pu} + \omega_s)^2 + \Gamma^2 \right\}} \quad (2)$$

The current state-of-the-art setup for heterodyne-detected CARS-ROA is reported by K. Hiramatsu et al.¹⁶ where narrowband pump (532 nm, ~ 100 mW) and broadband Stokes (around 545–590 nm, 20 mW) pulses, both in the visible region, at 25-kHz repetition rate were employed for CARS excitation. The use of 400-ps duration pump pulses kept the fluence at the sample low enough to reach the threshold for other unwanted nonlinear effects and guaranteed that the entire “temporally stretched” Stokes pulse remains temporally synchronized with the pump pulse to acquire broadband CARS spectra. Using this setup, heterodyne-detected CARS-ROA spectra of neat liquid enantiomers (+)- and (-)- β -pinene were acquired with 1 min of exposure time. The spectra show two times larger CARS-ROA-to-achiral CARS ratio as compared with those recorded with the setup¹⁴ excited by the pump/Stokes in the near-infrared (NIR) region. In another approach, an interferometric coherent Raman optical activity (iCROA) setup was built using NIR excitation where a generally weak CARS-ROA field of neat (-)- β -pinene liquid was amplified using interference with a local oscillator of achiral CARS field separately generated in water by a portion of the same NIR excitation.¹⁷

In this work, we present an experimental realization of heterodyne-detected CARS-ROA that uses a conventional broadband CARS setup with ~ 1 ps, 670 nm (or 800 nm) pump, and ~ 60 fs, 710 nm (or 850 nm) Stokes pulses at 20-kHz repetition rate. About 1 mW (or 1.2 mW) of pump and 4.5 mW (or 11 mW) of Stokes powers reach the sample. To the best of our knowledge, CARS-ROA spectroscopy has been shown for pure liquids such as β -pinene, but it has not yet been demonstrated for chiral molecules dissolved in an achiral solvent. Here, we show the first heterodyne-detected CARS-ROA spectra of a 2-M solution of either (R)- or (S)-2,2'-Bis-(methoxy)-1,1'-binaphthalin (MOM-BINOL) molecules (chiral) in dichloromethane (DCM, achiral). The acquired CARS-ROA spectra of (R/S)-MOM-BINOLs are in sufficiently

good agreement with the experimentally acquired spontaneous ROA spectra (with 532-nm cw laser excitation) of the same samples, and also with the DFT-calculated ROA spectra of the two atropisomers in DCM environment. To the best of our knowledge, these are the first experimentally acquired spontaneous ROA spectra of (R/S)-MOM-BINOLs. BINOL and its derivatives belong to a class of important compounds that have been widely used as organocatalysts in asymmetric synthesis. Especially, BINOL-phosphoric acids, which are chiral Brønsted acids, are widely used in asymmetric organocatalysis.⁹ Overall, our work presents the first CARS-ROA spectrum of an important chiral precursor for the synthesis of organocatalysts that is dissolved in an achiral solvent. We therefore extend the application of CARS-ROA from neat chiral liquids (earlier work) to chiral solutions (our work).

2 | MATERIAL AND METHODS

Figure 2 shows the schematics of our experimental setup for heterodyne-detected CARS-ROA spectroscopy. More details of the laser system for broadband CARS can be found elsewhere.¹⁸ Briefly, an amplified 6 W Yb-laser (PHAROS, Light Conversion) operating at 20-kHz synchronously pumps two independent nonlinear optical parametric amplifiers (OPAs; Orpheus-F, Light Conversion). Both OPAs are tunable in the wavelength range 640–940 nm and provide vertically polarized ~ 50 fs pulses with ~ 150 -mW average power. We used the conventional two-beam broadband CARS configuration in two different pump/Stokes wavelength combinations, namely, (1) 670-nm pump and 710-nm Stokes and (2) 800-nm pump and 850-nm Stokes, to acquire CARS-ROA spectra with “short wavelength” and “long wavelength” excitations, respectively. The output of the first OPA (OPA 1) operating at central wavelength 670 nm (or 800 nm) was spectrally filtered by a grating-based spectral filter to get ~ 1 ps (FWHM ~ 14 cm⁻¹) pulses to serve as narrowband pump. The output of the second OPA (OPA 2) operating at central wavelength 710 nm (or 850 nm) is used as broadband Stokes. The pump and Stokes pulses were temporally and spatially synchronized in a collinear geometry and focused on to the sample using an achromatic lens (L1; $f = 10$ cm). The liquid samples were kept in a 1-mm quartz cuvette (Hellma; 350 μ L). The entire available pump power (average powers: 670 nm, 1 mW; or 800 nm, 1.2 mW) was used; however, the Stokes power was kept low on the sample (average powers: 710 nm, ~ 4.5 mW; or 850 nm, ~ 11 mW) to prevent sample degradation and other undesired nonlinear effects. A high-quality Glan–Thompson prism polarizer

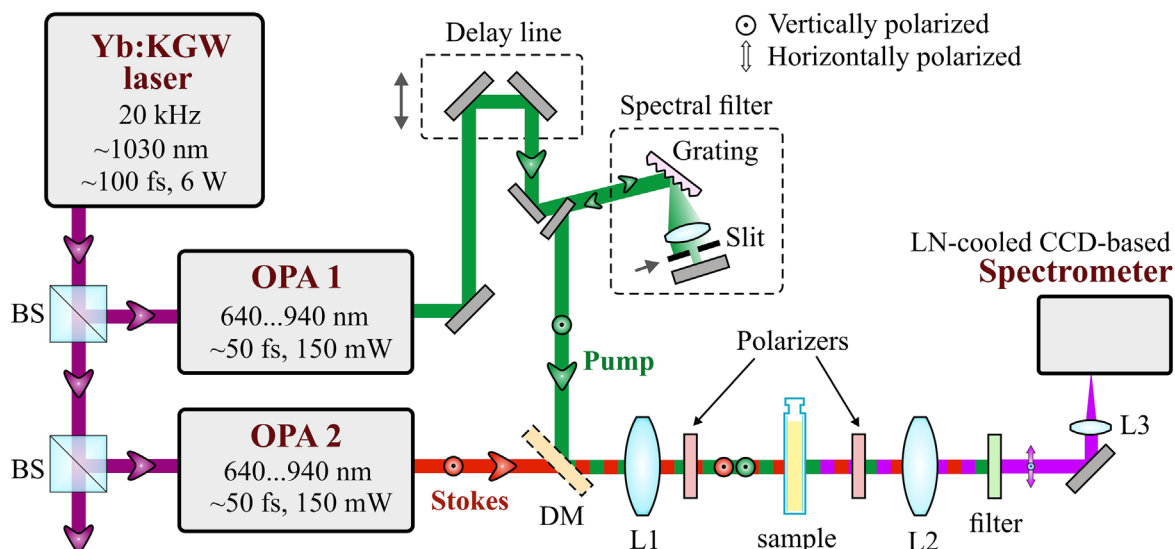


FIGURE 2 Schematic of the experimental setup for heterodyne-detected broadband CARS-ROA spectroscopy. BS, beam splitter; DM, dichroic mirror; L1 & L2, L3, lens.

(P1; B. Halle Nachfl. GmbH, extinction ratio $<10^{-8}$, prismatic deviation $<5''$) with its polarization axis oriented along the pump/Stokes polarizations was placed between the focusing lens and the sample to further purify the polarization of the input beams. The generated CARS signal was collected by another achromatic lens (L2; $f = 10$ cm), and the incident pump and Stokes wavelengths were spectrally filtered/blocked by two bandpass filters. Finally, the broadband CARS signal was focused ($f = 25$ cm lens) on the entrance slit of a 30-cm focal length polychromator (HORIBA Scientific; iHR320) equipped with a liquid nitrogen-cooled CCD (Symphony II). For heterodyne-detected CARS-ROA, a second high-quality Glan–Thompson prism polarizer (analyzer P2; B. Halle Nachfl. GmbH, the same type as P1 used in the excitation path), fixed on a high-precision motorized rotational mount (Standa Ltd.: model 8MPR16-1, step resolution 0.0125°), was placed between the cuvette and the collecting lens. The polarization axis of the analyzer was initially kept in the crossed position with respect to that of polarizer P1 in the excitation path. From this crossed position, the analyzer was slightly rotated to achieve the “maximum extinction position” for the anti-Stokes wavelengths. We have found that this “maximum extinction position” is sample-dependent because of intrinsic ORD from the sample. We determined a very low extinction ratio of $\sim 10^{-8}$ after the collecting lens for the entire anti-Stokes spectral region, which is crucial for suppressing the achiral CARS background and obtaining a sufficiently high-quality heterodyne-detected CARS-ROA spectrum. For this measurement, we first acquired the very weak residual achiral CARS signal at

the crossed analyzer position without any OD filters with an acquisition time of 10 s; then, we rotated the analyzer to the parallel position, added a set of OD filters yielding a total OD of 8 for attenuating the strong achiral CARS signal and recorded it with the same acquisition time as for the crossed position for direct comparison.

Two successive spectra for analyzer polarization axis at angles $\pm\theta$ with respect to the maximum extinction position were recorded. The intensity difference of the two spectra was computed to obtain the heterodyne-detected CARS-ROA spectrum.

Spectroscopic grade liquid (–) and (+)- β -pinene were purchased from Merck KGaA, Germany, and used without any further purification. Solid-state (*R*- and (*S*)-MOM-BINOLs were synthesized from (*R*)-BINOL and (*S*)-BINOL (purchased from RCA separations, each $>99.9\%$ ee) based on a literature procedure.¹⁹ Spectroscopy grade DCM was also purchased from Merck KGaA, Germany.

Spontaneous ROA spectra of (*R*- and (*S*)-MOM-BINOLs in DCM solutions were measured using a commercial ROA spectrometer (ChiralRaman-2X spectrometer, BioTools Inc.), with backscattering geometry, SCP configuration, 7-cm^{-1} resolution, $\sim 70\text{- to }2500\text{-cm}^{-1}$ measurement range, equipped with 532-nm laser line (Laser Quantum, Opus 532) and CCD camera detector (Critical Link, MityCCD-E3011BI-DVM). The laser power and accumulation time of single scan were set up to 30 mW and 0.5 s, respectively. Extended measurement range in the low wavenumber region was obtained using the ultrastep long-pass 532-nm RazorEdge Rayleigh filter from Semrock. The total acquisition time of each

sample was approximately 18 h. Particularly for these spontaneous ROA measurements, the 2 M solutions, after dissolving (*R*)- and (*S*)-MOM-BINOL in DCM (Avantor, 99.8%), were further purified by activated charcoal, followed by filtering (Millex-LG, PTFE, 0.20 μm , Millipore), and exposed for the incident laser radiation for 30 min in order to reduce the fluorescence background.

Spontaneous ROA spectra of (*R*)- and (*S*)-MOM-BINOLs were simulated using DFT calculations performed with the GAUSSIAN 2016 program (B3LYP functional and the 6-311++G(d,p) basis set, harmonic approximation, and incident frequency 14,992.5 cm^{-1}). A polarizable continuum model with the dielectric constant $\epsilon = 8.93$ of the solvent DCM was used. The peak positions of the calculated spectra are further corrected by a scaling factor of 0.9798. Final spectra were plotted with Lorentzian profiles (FWHM 6 cm^{-1}).

Spontaneous Raman spectra were acquired using a customized Raman spectrometer that comprises a 633-nm excitation by a HeNe laser, an inverted microscope (Nikon Eclipse Ti), and a 55-cm focal length polychromator (HORIBA Scientific, iHR550) equipped with a Peltier-cooled CCD (Synapse).

3 | RESULTS AND DISCUSSION

We first tested the heterodyne-detected CARS-ROA spectroscopy setup by acquiring heterodyne-detected CARS-ROA spectra of (*-*)- β -pinene and (*+*)- β -pinene that are liquids at room temperature. Earlier work on spontaneous ROA on (*-*)- β -pinene²⁰ suggests that two peaks at 716 and 765 cm^{-1} are dominant in forward scattering. For reproducing the pioneering CARS-ROA work from Hiramatsu et al.,¹⁴ we also chose the spectral region from 500 to 1250 cm^{-1} . The broadband Stokes pulses were tuned to approximately 710 nm, whereas the narrowband pump was centered at 670 nm. The measured CARS-ROA spectrum of (*+*)- β -pinene enantiomer is depicted in Figure 3. It is the difference of the two heterodyne-detected CARS spectra at analyzer positions $\theta = \pm 0.11^\circ$ obtained in 1-min acquisition time each. There are two possible ways to obtain the difference spectrum, namely, (1) heterodyne-detected CARS spectrum obtained at $+\theta$ position minus the heterodyne-detected CARS spectrum obtained at $-\theta$ and (2) heterodyne-detected CARS spectrum obtained at $-\theta$ position minus the heterodyne-detected CARS spectrum obtained at $+\theta$, and the two ways would give two CARS-ROA spectra with oppositely signed peaks. Therefore, it is important to fix the sign convention and figure out the appropriate way that would provide the correctly signed peaks for the CARS-ROA spectrum of an optical isomer. In our setup, we found out that if we look at the

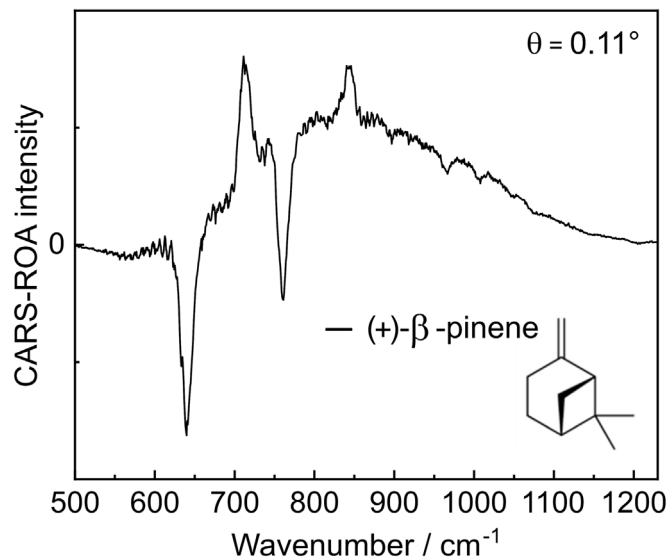
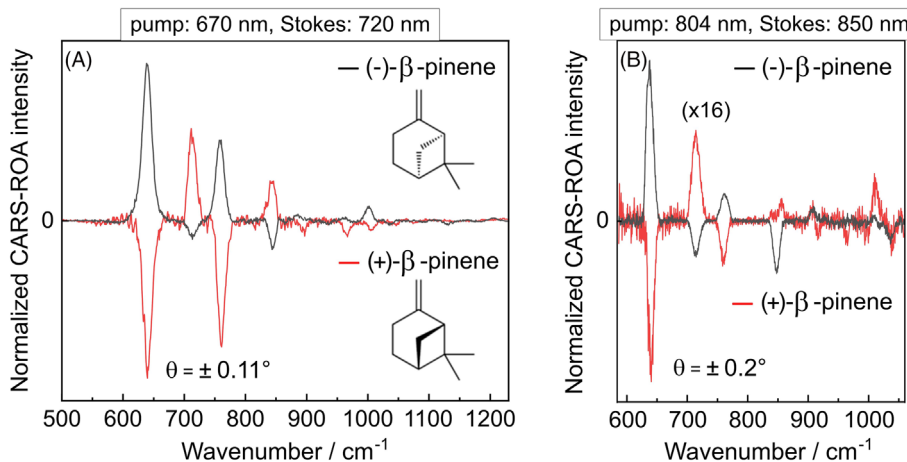


FIGURE 3 Experimentally acquired heterodyne-detected CARS-ROA spectrum of (*+*)- β -pinene neat liquid obtained as difference spectrum acquired at $\theta = \pm 0.11^\circ$. It has hilly background due to residual achiral signal.

analyzer from the sample side and take the anticlockwise rotation of the analyzer as $+\theta$, then option (1) provides the peak positions and their signs in good agreement with previously reported spectra of β -pinene enantiomers.^{14,16,20,21} The spectrum shows a hilly background that arises from purely electronic contributions termed “non-Raman-resonant background”; it arises, for example, from the solute, the solvent, and the cuvette material. In an ideal situation, where $|+\theta| = |-\theta|$, the residual CARS signal should be completely removed by subtracting the two spectra. We attribute the residual background in Figure 3 to the experimentally limited minor differences between $|+\theta|$ and $|-\theta|$; it can be removed by subtraction of a baseline after spline fitting. To take care of CARS signal dependence on the Stokes spectral profile (Figure S1), each acquired CARS spectrum is normalized by the intensity profile of a non-resonant four-wave-mixing (FWM) signal from water acquired in the same experimental conditions. The background-free CARS-ROA spectrum retrieved from the spectrum in Figure 3 after spline fitted baseline removal is shown in Figure 4A, red curve, along with the CARS-ROA spectrum of (*-*)- β -pinene, Figure 4A black curve, obtained by the same procedure.

As can be seen, the two CARS-ROA spectra show oppositely signed vibrational peaks, which is a characteristic of ROA spectra of enantiomers. Four prominent peaks around 640, 715, 761, and 845 cm^{-1} are clearly seen. Their peak positions vary slightly from those reported in the spontaneous ROA spectra of Wilson.²¹ Generally, CARS lineshapes are much more complex

FIGURE 4 Heterodyne-detected CARS-ROA spectra of neat liquids (–)- β -pinene and (+)- β -pinene (A) with pump 670 nm and Stokes 710 nm excitation, and (B) with pump 800 nm and Stokes 850 nm excitation. The intensities in (B) are scaled by 16 to plot those in the same scale of the intensities in (A).



than those observed in the corresponding spontaneous/linear Raman spectrum because of the coherent mixing of the Raman-resonant and the non-Raman-resonant contributions, giving rise to complex dispersive lineshapes. Therefore, peak positions in CARS and Raman spectra usually differ. The larger the non-Raman-resonant background, the larger is this discrepancy. In heterodyne-detected CARS-ROA, a small fraction of the achiral contribution (Raman-resonant signal plus non-Raman-resonant background) passes the analyzer at $|\theta|$ and $|\theta|$, respectively, and interferes with the chiral-CARS signal. Small discrepancies between $|\theta|$ and $|\theta|$ may therefore lead to differences in both peak positions and intensities for the two enantiomers.

We also acquired the heterodyne-detected CARS-ROA spectra of the same (–)– and (+)– β -pinene liquids using “long wavelength” excitations, pump: 800 nm and Stokes 850 nm, at analyzer positions $\theta = \pm 0.2^\circ$ with ~ 5 min per spectral acquisition (cf. Figure 4B). The positions and the orientations of the peaks in the spectra are sufficiently well-matched with the corresponding CARS-ROA spectra of β -pinenes obtained using “short wavelength” excitations. However, despite using higher pump (1.2 mW) and Stokes (11 mW) powers, higher throughput of the analyzer ($\theta = \pm 0.2^\circ$), and longer acquisition times as compared with those used for acquisitions at “short wavelength” excitation, the intensities in the spectra acquired using “long wavelength” excitations are found to be 16 times small as compared with those obtained by “short wavelength” excitations. This might be due to the fact that the ROA intensities are inversely proportional to the fifth power of the excitation wavelength.

Next, we applied the setup for acquiring the heterodyne-detected CARS-ROA spectra of separate solutions (2 M) of enantiomers, (*R*)-MOM-BINOL and (*S*)-MOM-BINOL in DCM. Following the same procedure for obtaining the difference spectrum as we did for β -pinene enantiomers, the CARS-ROA spectra of MOM-BINOL

enantiomers in DCM solutions are obtained in 4 min of acquisition time each, at $\theta = \pm 0.4^\circ$ positions of the analyzer. About 1 mW of pump (670 nm) and 10 mW of Stokes (730 nm) powers were used at the sample. The two CARS-ROA spectra are depicted in Figure 5B. To the best of our knowledge, these are the first experimentally acquired CARS-ROA spectra of chiral molecules dissolved in an achiral solvent. We clearly see the oppositely signed peaks at 1018 [1019], 1140 [1145], 1376 [1375], and 1434 [1432] cm^{-1} positions in (*R*)-MOM-BINOL [(*S*)-MOM-BINOL] spectra. Figure 5A top shows the calculated spontaneous ROA spectra of the MOM-BINOL atropisomers in the DCM environment, and Figure 5B bottom is the experimentally acquired spontaneous ROA spectra of the same solutions of MOM-BINOL atropisomers in the DCM. The DFT calculations assign the most intense peak at 1376 [1375] cm^{-1} in the observed CARS-ROA spectra to the symmetric and the asymmetric ring stretching modes of the naphthalene ring. The DFT-calculated vibrational mode assignments to the other prominent modes in the spectral range of 670–1600 cm^{-1} are presented in Table S1. The peak positions of most of the dominant peaks and their signs in both the experimental spontaneous ROA and the heterodyne-detected CARS-ROA spectra are in sufficiently good agreement. We do see oppositely signed peaks in each of the heterodyne-detected CARS-ROA spectra. The modes both at the far-left and the far-right sides in the CARS-ROA spectra are not observed because of very low intensities at the wings of the Stokes intensity profile. Again, please note the two orders of magnitude for the acquisition times of the spontaneous ROA (18 h = 1080 min) as compared with CARS-ROA (8 min).

Furthermore, in order to demonstrate the enantio-sensitivity of our heterodyne-detected CARS-ROA setup that whether it selectively observes the vibrational modes (Raman peaks) of MOM-BINOL chiral molecules in the presence of the achiral solvent molecules (DCM)

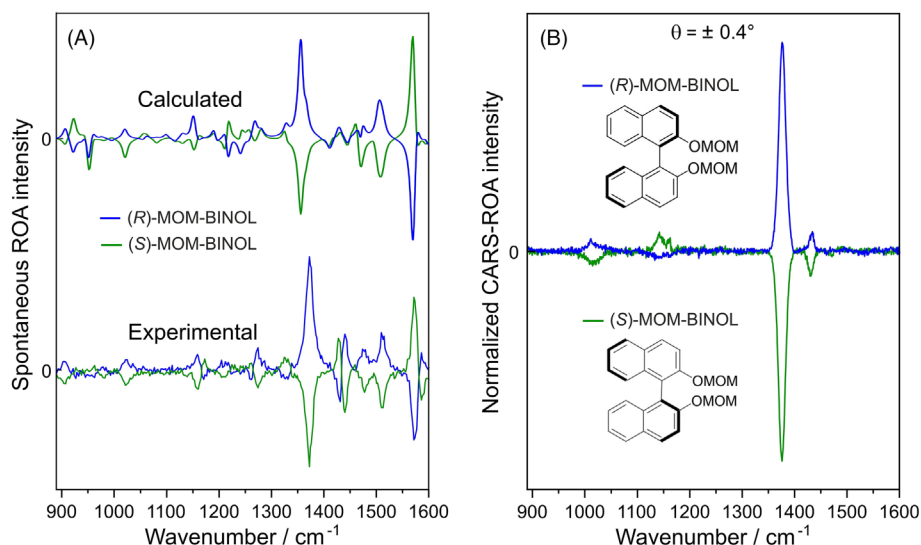


FIGURE 5 (A) Upper spectra: the DFT-calculated spontaneous ROA spectra of (*R*)-MOM-BINOL (blue curve) and (*S*)-MOM-BINOL (green curve) molecules in DCM environment; lower spectra: the experimentally acquired spontaneous ROA spectra of 2 M solutions of (*R*)-MOM-BINOL (blue curve) and (*S*)-MOM-BINOL (green curve) molecules in DCM; (B) heterodyne-detected CARS-ROA spectra of 2 M solutions of (*S*)-MOM-BINOL (green curve) and (*R*)-MOM-BINOL (blue curve) molecules in DCM. The peaks at 1018 [1019], 1140 [1145], 1376 [1375], and 1434 [1432] cm^{-1} of (*R*)-MOM-BINOL [(*S*)-MOM-BINOL] in (B) exhibit opposite signs. The Raman peaks of the achiral solvent (DCM) are not observed.

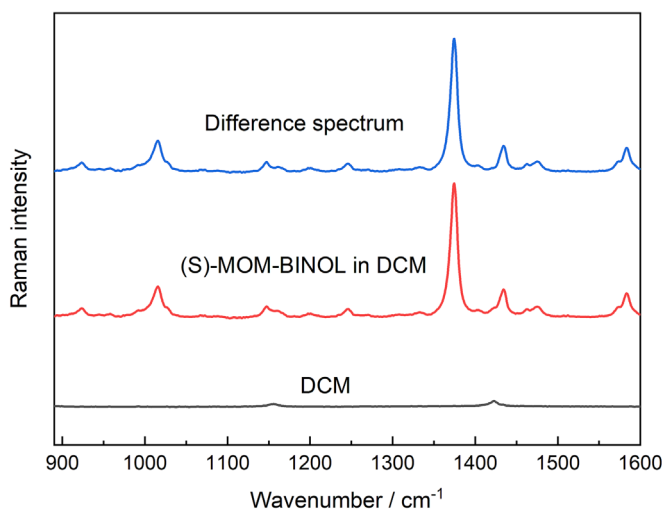


FIGURE 6 Spontaneous Raman spectra of (*R*)-MOM-BINOL in DCM (2 M) solution (in red) and pure DCM (in black). The blue curve is the difference spectrum of the red (solution) and the black (solvent) spectra.

or not, we have acquired spontaneous Raman spectra of the same 2 M solution of (*S*)-MOM-BINOL in DCM (Figure 6, middle curve) and of a neat DCM (Figure 6, bottom curve), respectively. The difference spectrum of the two acquired spectra represents the Raman spectrum of (*S*)-MOM-BINOL molecules only (Figure 6, top curve) under the reasonable assumption that both solute and solvent do not show significant intermolecular

interactions. The prominent peaks around 1017, 1147, 1374, and 1434 cm^{-1} in this spectrum can be easily related to peaks at 1019, 1145, 1375, and 1432 cm^{-1} , respectively, observed in the CARS-ROA spectrum of (*S*)-MOM-BINOL. Interestingly, as expected, the Raman bands of achiral DCM molecules, which are present around 1156 and 1423 cm^{-1} , respectively, in both the Raman spectrum of (*S*)-MOM-BINOL in DCM solution and the Raman spectrum of neat DCM, are automatically absent in the CARS-ROA spectrum without any “post-processing.” However, a post-processing was needed to achieve the blue spectrum in Figure 6 in the spontaneous Raman case. This confirms the enantiosensitivity of heterodyne-detected CARS-ROA spectroscopy.

It is worth mentioning that the current state-of-the-art heterodyne-detected CARS-ROA spectroscopy setups including this work are prone to have artifacts in the spectrum. There are a few important factors contributing to these artifacts. First, the subtraction of the two heterodyne-detected CARS spectra at $\pm\theta$ positions of the analyzer often does not cancel out completely the homodyne terms, the first and second terms of Equation (1), that contain achiral CARS-like slightly blue-shifted dispersive bands. Even tiny contributions of these terms give rise to background in the CARS-ROA spectrum, spectrally shifted CARS-ROA bands and sometimes also artificial peaks. The perfect cancellation of the homodyne terms is subject to the exact determination of the $\theta = 0^\circ$ position of the analyzer. However, it is challenging to

achieve this when the chiral-CARS-to-achiral-CARS background ratio is small, which is generally the case for diluted solutions of chiral molecules in achiral solvents. The situation is complicated further due to the presence of ORD, a linear but not a Raman-induced effect by chiral molecules, that gives a sample-dependent (and also concentration-dependent) polarization rotation for the CARS field. The ORD gives the equal and opposite shifts of zero-positions for the same concentrations of the two enantiomers with respect to $\theta = 0^\circ$ position for an achiral sample like most solvents. The second origin of artifacts is the first term in the square brackets of Equation (3) that also contributes to the heterodyne term^{14,15}:

$$\begin{aligned} \Delta I(\omega_{aS}) &\equiv I(\omega_{aS}, \theta) - I(\omega_{aS}, -\theta) \\ &\propto 4 \cos \theta \sin \theta A \cdot \left[\frac{\chi_{2111,Im}^{(3)NR} \cdot N I}{2 \hbar \left\{ (\Omega - \omega_{pu} + \omega_S)^2 + \Gamma^2 \right\}} \right. \\ &\quad \left. + \frac{I_{CID}^{sp. ROA}(0^\circ) \cdot \chi_{1111}^{(3)NR} \cdot N I / 2}{2 \hbar \left\{ (\Omega - \omega_{pu} + \omega_S)^2 + \Gamma^2 \right\}} \right] \end{aligned} \quad (3)$$

where $\chi_{2111,Im}^{(3)NR}$ is the non-resonant part of the corresponding susceptibility tensor component and is a mathematically “real” quantity. This additional term gives the bands of the spontaneous Raman spectrum weighted by $\chi_{2111,Im}^{(3)NR}$ and is achiral in nature. Because $\chi_{2111}^{(3)} \ll \chi_{1111}^{(3)}$, this term is quite small for neat chiral liquids like β -pinenes and can be neglected. However, it cannot be completely ignored for diluted chiral samples like MOM-BINOL enantiomers in DCM. The achiral background without artificial peaks and spectral peak shifts can be removed by subtracting a spline-fitted baseline to the background. However, the elimination of such artifacts like spectral peak shifts and artificial peaks is not straightforward. We have observed residual achiral backgrounds in all the CARS-ROA spectra of β -pinenes liquids and 2 M MOM-BINOL enantiomer solutions presented here. Fortunately, we have not seen artifacts like spectral shifts, possibly they are negligible, and artificial peaks in all of them. Therefore, we corrected them by spline-fitted baseline removal as discussed above.

4 | CONCLUSIONS

We have demonstrated a heterodyne-detected CARS-ROA spectroscopy setup that is built up on a conventional broadband CARS spectroscopy setup. It requires low average powers, about 1 mW (or 1.2 mW) and 4.5 mW (or 11 mW) of ~ 1 -ps pump pulses and ~ 60 -fs

Stokes pulses, respectively, at the sample for the “short wavelength” (or the “long wavelength”) excitation. With this arrangement, we have shown sufficiently good quality heterodyne-detected CARS-ROA spectra of β -pinene chiral isomers each recorded in similar acquisition times (1 min) as reported in previous works on CARS-ROA^{14,16} that have used much longer duration pump and Stokes pulses with significantly higher average powers of 100 mW (pump) and 20 mW (Stokes) at the sample. In a step further, we have shown here the first experimental CARS-ROA spectra of chiral molecules, that is, (*S/R*)-MOM-BINOLs, in the presence of achiral solvent molecules. These spectra were acquired in 4 min of acquisition times using the same powers and pulse durations of the pump and Stokes pulses. Chiral MOM-BINOLs serve as precursor molecules in the synthesis of an important class of chiral organocatalysts that are used in asymmetric reactions to create chiral products in bulk. Hence, these results are a step toward the application of coherent ROA in monitoring the asymmetric reactions catalyzed by these chiral organocatalysts. However, the concentration of 2 M employed in this study is clearly too high for a real organocatalytic reaction where reagent/product concentrations are often in the mM range and catalyst concentrations even lower. In its present form, CARS-ROA is unfortunately not capable of monitoring organocatalysis on practically relevant time scales. It needs further development to demonstrate artifacts-free coherent ROA of low concentrations of chiral molecules in achiral solvents. One possible approach we suggest is to incorporate a nonlinear non-resonant background (NRB) removal technique that still provides amplification of the chiral-CARS field with respect to the achiral-CARS field.






ACKNOWLEDGMENTS

V. K. acknowledges support by the German Research Foundation (Deutsche Forschungsgemeinschaft, DFG) under project number 511625800. Open Access funding enabled and organized by Projekt DEAL.

CONFLICT OF INTEREST STATEMENT

The authors declare no competing financial interest.

ORCID

Vikas Kumar  <https://orcid.org/0000-0002-7335-0824>
 Grzegorz Zajac  <https://orcid.org/0000-0003-4090-9334>
 Agnieszka Domagała  <https://orcid.org/0000-0003-2940-4933>
 Małgorzata Barańska  <https://orcid.org/0000-0001-8826-3144>
 Sebastian Schlücker  <https://orcid.org/0000-0003-4790-4616>

REFERENCES

- [1] L. A. Nafie, J. C. Cheng, P. J. Stephens, *J. Am. Chem. Soc.* **1975**, 97(13), 3842. <https://doi.org/10.1021/ja00846a061>
- [2] L. A. Nafie, T. A. Keiderling, P. J. Stephens, *J. Am. Chem. Soc.* **1976**, 98(10), 2715. <https://doi.org/10.1021/ja00426a007>
- [3] L. D. Barron, M. P. Bogaard, A. D. Buckingham, *J. Am. Chem. Soc.* **1973**, 95(2), 603. <https://doi.org/10.1021/ja00783a058>
- [4] L. D. Barron, M. P. Bogaard, A. D. Buckingham, *Nature* **1973**, 241(5385), 113. <https://doi.org/10.1038/241113a0>
- [5] F. Zhu, N. W. Isaacs, L. Hecht, L. D. Barron, *Structure* **2005**, 13(10), 1409. <https://doi.org/10.1016/j.str.2005.07.009>
- [6] A. G. Berkessel, *Harald asymmetric organocatalysis: from biomimetic concepts to applications in asymmetric synthesis*, Wiley-VCH, Weinheim **2005**.
- [7] A. Erkkilä, I. Majander, P. M. Pihko, *Chem. Rev.* **2007**, 107(12), 5416. <https://doi.org/10.1021/cr068388p>
- [8] S. Mukherjee, J. W. Yang, S. Hoffmann, B. List, *Chem. Rev.* **2007**, 107(12), 5471. <https://doi.org/10.1021/cr0684016>
- [9] D. Parmar, E. Sugiono, S. Raja, M. Rueping, *Chem. Rev.* **2014**, 114(18), 9047. <https://doi.org/10.1021/cr5001496>
- [10] J. Ö. Bjarnason, H. C. Andersen, B. S. Hudson, *J. Chem. Phys.* **1980**, 72(7), 4132. <https://doi.org/10.1063/1.439642>
- [11] L. D. Barron, A. D. Buckingham, *J. Chem. Soc., Chem. Commun.* **1973**, 5, 152. <https://doi.org/10.1039/C39730000152>
- [12] H. Boucher, T. R. Brocki, M. Moskovits, B. Bosnich, *J. Am. Chem. Soc.* **1977**, 99(21), 6870. <https://doi.org/10.1021/ja00463a014>
- [13] J. L. Oudar, C. Minot, B. A. Garetz, *J. Chem. Phys.* **1982**, 76(5), 2227. <https://doi.org/10.1063/1.443296>
- [14] K. Hiramatsu, M. Okuno, H. Kano, P. Leproux, V. Couderc, H.-o. Hamaguchi, *Phys. Rev. Lett.* **2012**, 109(8), 083901. <https://doi.org/10.1103/PhysRevLett.109.083901>
- [15] V. Kumar, S. Schlücker, Chapter 4—Coherent chiroptical Raman spectroscopy, in *Molecular and Laser Spectroscopy*, (Ed: V. P. Gupta), Elsevier, Amsterdam **2022**, 101.
- [16] K. Hiramatsu, P. Leproux, V. Couderc, T. Nagata, H. Kano, *Opt. Lett.* **2015**, 40(17), 4170. <https://doi.org/10.1364/OL.40.004170>
- [17] K. Hiramatsu, H. Kano, T. Nagata, *Opt. Express* **2013**, 21(11), 13515. <https://doi.org/10.1364/OE.21.013515>
- [18] S. Küpper, V. Kumar, S. Schlücker, *J. Phys. Chem. A* **2019**, 123(29), 6291. <https://doi.org/10.1021/acs.jpca.9b05142>
- [19] T. R. Wu, L. Shen, J. M. Chong, *Org. Lett.* **2004**, 6(16), 2701. <https://doi.org/10.1021/ol0490882>
- [20] L. D. Barron, L. Hecht, A. R. Gargaro, W. Hug, *J. Raman Spectrosc.* **1990**, 21(6), 375. <https://doi.org/10.1002/jrs.1250210609>
- [21] H. W. Wilson, *Appl. Spectrosc.* **1976**, 30(2), 209. <https://doi.org/10.1366/000370276774456282>

SUPPORTING INFORMATION

Additional supporting information can be found online in the Supporting Information section at the end of this article.

How to cite this article: V. Kumar, T. Reichenauer, L. Supovec, D. Jansen, N. Brodt, G. Zając, A. Domagała, M. Barańska, J. Niemeyer, S. Schlücker, *J Raman Spectrosc* **2023**, 54(9), 1011. <https://doi.org/10.1002/jrs.6575>



EDINBURGH
INSTRUMENTS

New eBook Out Now!



Scan to download
the new eBook...

Discover the ways we can enhance your research
with multiple techniques in one instrument

Multimodal Imaging Raman and Beyond

edinst.com

